Available online at www.sciencedirect.com
SCIENCE DIRECT®
Materials Chemistry and Physics 82 (2003) 786–792
MATERIALS CHEMISTRY AND PHYSICS
www.elsevier.com/locate/matchemphys

Corrosion behaviour of 304 stainless steel in sulphuric acid solutions and its inhibition by some substituted pyrazolones

M. Abdallah

Chemistry Department, Faculty of Science, Benha University, Benha, Egypt

Received 18 February 2003; received in revised form 1 July 2003; accepted 11 July 2003

Abstract

The corrosion behaviour of 304 stainless steel (SS) in 0.5 M H_2SO_4 solution was studied using potentiodynamic and galvanostatic polarization techniques. Three anodic peaks were observed in the potentiodynamic anodic polarization curves before oxygen evolution. The effects of acid concentrations and voltage scan rate were studied. The inhibitive effect of 4-substituted pyrazole-5-ones toward the corrosion of 304 SS in 0.5 M H_2SO_4 were studied. The inhibition action of these compounds was assumed to occur via adsorption on the steel surface through the active centres contained in their structure. The mechanism of inhibition was interpreted on the basis of the inductive and mesomeric effects of the substituents. There is a good agreement between the percentage inhibition efficiencies calculated from both techniques. The inhibition efficiencies increase with increasing the inhibitor concentrations.

Keywords: 304 stainless steel; Pyrazole-5-one; Inhibition

1. Introduction

The corrosion of stainless steel (SS) in acidic solutions is a fundamental academic and industrial concern that has received a considerable amount of attention. The most important fields of application being acid pickling, industrial acid cleaning, acid descaling and oil well acidizing. Because of the general aggressiveness of acid solutions, inhibitors commonly used to reduce the corrosion attack on metallic materials.

Organic adsorption compounds are effective as corrosion inhibitors for corrosion of different types of SSs in acidic medium because of the functional group containing hetero atoms such as nitrogen, sulphur and oxygen [1–5]. The inhibitive properties arise from their ability to be adsorbed onto the electrode surface. The relation between the chemisorption inhibition mechanism and variation in the electronic structure of the inhibitor has been studied [6–10].

The present work is devoted to investigate the corrosion behaviour of 304 SS in H_2SO_4 solutions over a certain range of concentration and scan rate using potentiodynamic and galvanostatic polarization techniques. The effect of addition of four derivatives of 4-substituted pyrazole-5-one compounds as corrosion inhibitors was examined in 0.5 M H_2SO_4.

2. Experimental

The sample was 304 SS electrode having the chemical composition (18.18% Cr, 8.48% Ni, 1.75% Mn, 0.5% Si, 0.36% Mo, 0.051% C, 0.05% N, 0.005% S, 0.028% P and the remainder is Fe). The bottom end of the rod specimen with a mean surface area of 0.68 cm^2 was successively abraded with 1-, 0- and 00-emery paper, degreased with acetone and dried between two filter papers then immersed in 50 ml of the test solution. All chemicals used were of AR quality. The solutions were prepared using bidistilled water. No attempts were made to deareate them. The electrolytic cell was all Pyrex glass and is described elsewhere [11].

Potentiodynamic anodic polarization curves were performed using a Wenking potentioscan. Type POS-73. The current density–potential curves were recorded on *X–Y* recorder type PL-3. All experiments were carried out at 25 ± 1 °C. Polarized atomic absorption spectroscopy (Z-6001) was used for determination of iron, chromium and nickel in the test solution after complete electrolysis at each peak.

Galvanostatic polarization studies were carried out using EG & G model 173 potentiostat/galvanostat. Three

E-mail address: metwally552@hotmail.com (M. Abdallah).

0254-0584/$ – see front matter © 2003 Elsevier B.V. All rights reserved.
doi:10.1016/S0254-0584(03)00367-5

compartment cell with a saturated calomel reference electrode and a platinum foil auxiliary electrode was used.

2.1. Materials

The chemical structure of 4-substituted pyrazole-5-ones are:

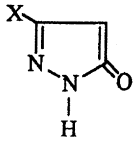

where X is equal to Cl, CH_3, CH_2CH_3 and OCH_3 for compounds I, II, III and IV, respectively.

3. Results and discussion

3.1. Potentiodynamic polarization measurements

Fig. 1 represents the potentiodynamic anodic polarization of 304 SS in 0.5 M H_2SO_4 solution. The starting potential was −1.0 V (SCE) and the scan range extended up to +2 V at a voltage scan rate of 50 mV s^{-1}. Inspection of Fig. 1 reveals the following features: four anodic regions labelled (A–D) before oxygen evolution takes place. These are: the anodic peaks (A) and (B) followed by a passive region (C) and finally the anodic peak (D). The first anodic peak (A) occurs at about −0.25 V (SCE). At this potential the formation of Fe, Cr and Ni oxides is expected due to the occurrence of their equilibria at potential range more negative than this potential [12]. One or more of the following reactions may occur under peak (A)

$$Fe + H_2O \rightarrow FeO + 2H^+ + 2e \quad (1)$$

$$Ni + H_2O \rightarrow NiO + 2H^+ + 2e \quad (2)$$

$$Cr + H_2O \rightarrow CrO + 2H^+ + 2e \quad (3)$$

The dissolution rate at peak (A) potential increases with increasing of both the acid concentration and the voltage scan rate as shown in Figs. 2 and 3. On the other hand, investigation of Table 1 reveals that, iron ions can be detected and measured by atomic absorption analysis. While, no chromium or nickel ions could be detected from dissolution of 304 SS during this anodic step and could not detected in the solution. These observations suggest that the formation of iron hydroxide takes place through the dissolution–precipitation mechanism in which the formed compound is soluble in the surrounding medium and starts to deposit on the electrode surface when its solubility

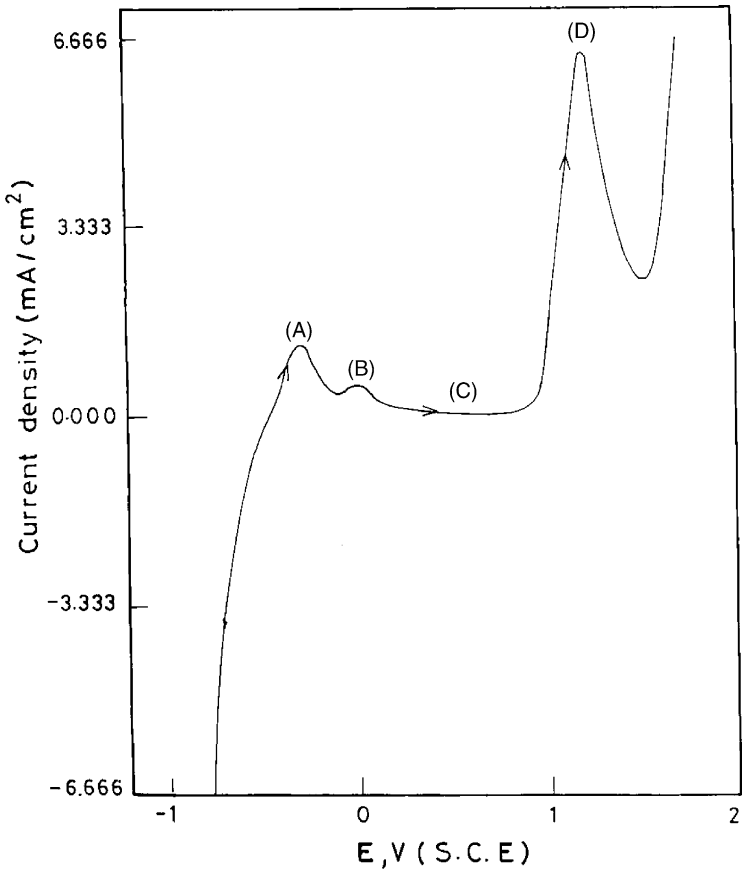

Fig. 1. Potentiodynamic anodic polarization of 304 SS electrode in 0.5 M H_2SO_4 at a scan rate of 50 mV s^{-1}.

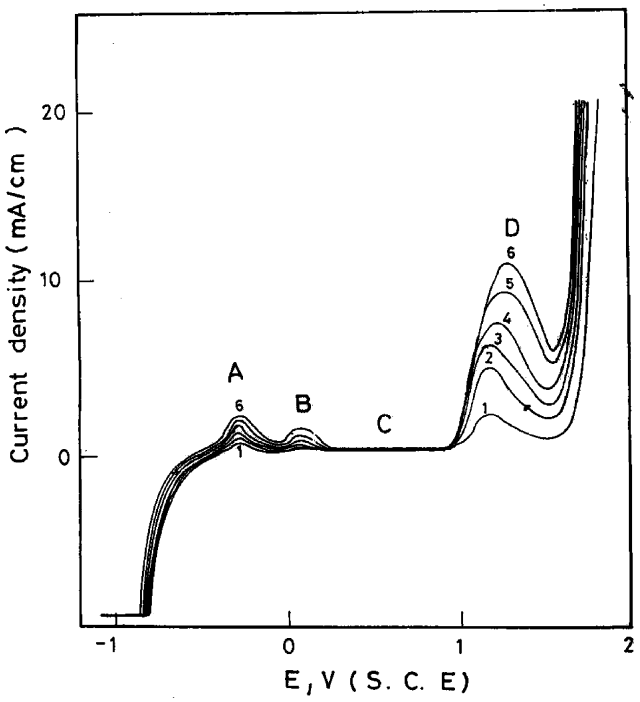

Fig. 2. Effect of H_2SO_4 concentrations on the potentiodynamic anodic polarization of 304 SS electrode at a scan rate of 50 mV s^{-1}: (1) 0.1 M, (2) 0.3 M, (3) 0.5 M, (4) 0.7 M, (5) 0.9 M, (6) 1.0 M.

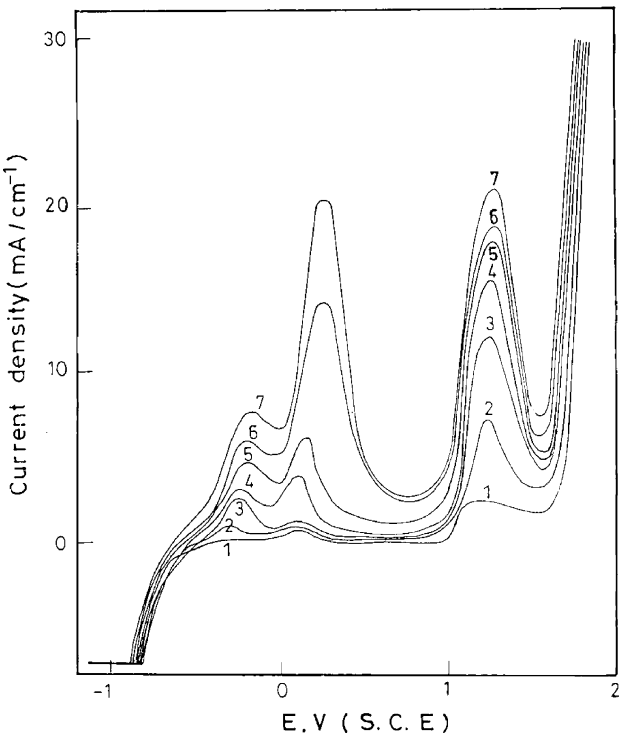

Fig. 3. Effect of different scan rates on the potentiodynamic anodic polarization of 304 SS in 0.5 M H_2SO_4: (1) 10 mV s^{-1}, (2) 50 mV s^{-1}, (3) 100 mV s^{-1}, (4) 250 mV s^{-1}, (5) 500 mV s^{-1}, (6) 750 mV s^{-1}, (7) 1000 mV s^{-1}.

product is exceeded. On the other hand, the formation of both chromium and nickel oxides takes place by direct nucleation and growth mechanism on the electrode surface and hence no chromium or nickel ions could be detected in the solution.

The second anodic peak (B) occurs at potential of −0.1 V (SCE). The formation of higher oxides of iron and chromium is expected as well as some thickening of nickel oxide:

$$2FeO + H_2O \rightarrow Fe_2O_3 + 2H^+ + 2e \quad (4)$$

$$2CrO + H_2O \rightarrow Cr_2O_3 + 2H^+ + 2e \quad (5)$$

Owing to its passivating properties and its resistance to acid solution, the chromium oxide (Cr_2O_3) is considered the main passive component in the formed film. Thus the anodic peak (B) is considered to be the main passive step in the anodic polarization of the SS. It is of interest to note that after the end of peaks (B) the anodic current starts to fall down and acquires its minimum value for a long potential period forming an passive region C. Along the region (C), the only reaction occurs is the thickening of the passive film as the applied anodic potential is increased. It is of interest to note that, the current flowing along the passive region is independent of the acid concentration whereas it increases markedly as the scan rate is increased.

The last anodic step before oxygen evolution which is a well defined peak (D) appears at +1.2 V (SCE). The formation of iron, nickel and chromium oxyhydroxides may take place at this potential range [13]. This peak acquires a large quantity of electricity indicating high dissolution of SS at its potential. Inspection of Table 1 reveals that, the concentration of Fe ion decreases at peek (D) potential while those of Ni and Cr increase. The anodic peek (D) represents the transpassive region where the formed passive film reacts with the medium forming soluble species with higher valences. Since the main passive film contains mainly Ni and Cr compounds which indirect contact with the aggressive solution, it is more likely that the concentration of their ions are increased in the test solution. At this potential Fe is protected by these films and the dissolution rate is expected to be decreased.

Table 1
Concentration of ionic species (ppm) as obtained from atomic absorption measurements at the anodic peak potential of 304 SS in 0.5 M H_2SO_4

Peak	Fe (ppm)	Ni (ppm)	Cr (ppm)
A	16.5	–	–
B	15.5	3	6.4
D	13.5	6.5	8.2

3.1.1. Effect of acid concentrations

Fig. 2 shows the effect of sulphuric acid concentration on the potentiodynamic anodic polarization curves of 304 SS at a scan rate of 50 mV s^{-1}. Table 2 illustrates the effect of the acid concentrations on peak potential E_p of peaks A, B and D and peak current densities i_p of A, B and D. Careful examination of Fig. 2 and Table 1 reveals that an increase

Table 2
Effect of acid concentration on peak potential (E_p) and peak current density (i_p) for peaks A, B and D at scan rate of 50 mV s^{-1}

Acid concentration (M)	E_p (mV, SCE)			i_p (mA cm^{-2})		
	A	B	D	A	B	D
0.1	−0.24	0.090	1.18	0.66	0.40	1.20
0.3	−0.25	0.100	1.22	0.02	0.60	5.80
0.5	−0.25	0.100	1.26	1.20	0.80	6.60
0.7	−0.26	0.120	1.30	1.40	0.90	7.60
0.9	−0.24	0.130	1.36	1.80	1.00	9.20
1.0	−0.25	0.140	1.40	2.10	1.02	10.90

of the acid concentration leads to: (i) the peak potential E_p of peak A is nearly constant while E_p for peaks B and D are shifted to more positive potential; (ii) the values of i_p for peaks A, B and D are increased with the acid concentration.

3.1.2. Effect of voltage scan rate

Fig. 3 shows the effect of variation of the voltage scan rate ν (10–1000 mV s^{-1}) on the potentiodynamic anodic polarization curves of 304 SS in 0.5 M H_2SO_4.

Table 3 shows the effect of voltage scan rate on E_p of peaks A, B and D and peak current density i_p of peaks A, B and D.

From inspection of Table 3, its clear that, an increase in voltage scan rate, the peak potential E_p for peaks A, B and D are shifted to more positive potentials. The positive shift in E_p could be explained on the basis of assumption that the time allowed to nucleation (growth) of oxides crystal is short and passivation is delayed until the nuclei have grown to critical size required for passivation [14]. These results are consistent with Muller's theory [15] where at higher scan rates, the electrical charge required to passivate the anode cannot be supplied completely and consequently, there is an increase in i_p as shown in Table 3.

Further inspection of the values in Table 3 reveals that as the voltage scan rate is increased i_p for all peaks are increased.

The extent of the passivation plateau (C) decreases as the scan rate is increased. This observation could be explained on the basis of another important effect of increasing voltage scan rate. In case of high scan rate, i.e. >100 mV s^{-1}, the magnitude of current peak (B) becomes larger than that of peak (A). This result leads to conclude that beside the formation of higher oxides from lower one (formed under peak A), there is also a large dissolution of the alloy under peak (B) to form the same higher oxides. Thus the formation of large quantities of the higher oxides occurs under peak (B). This relatively high oxide formation rate results in random deposition of the film component in wrong sites on the electrode surface and consequently a bad passivation properties of the film are obtained.

Table 3
Effect of voltage scan rate on peak potential (E_p) and peak current density (i_p) for peaks A, B and D

ν (mV s^{-1})	E_p (mV, SCE)			i_p (mA cm^{-2})		
	A	B	D	A	B	D
10	−0.35	0.10	1.20	0.10	0.20	1.60
50	−0.25	0.10	1.26	1.20	0.80	6.60
100	−0.20	0.10	1.28	2.60	1.50	11.20
250	−0.18	0.12	1.30	3.00	4.00	15.80
500	−0.20	0.22	1.33	4.80	5.90	17.20
750	−0.18	0.36	1.35	6.00	14.20	18.00
1000	−0.16	0.42	1.36	7.80	20.80	21.00

3.1.3. Effect of addition of 4-substituted pyrazole-5-ones

The effect of addition of increasing concentrations of 4-substituted pyrazole-5-ones on the potentiodynamic anodic polarization curves of 304 SS electrode in 0.5 M H_2SO_4 at a scan rate 50 mV s^{-1} was studied.

Fig. 4 shows typical potentiodynamic anodic polarization curves of 304 SS in 0.5 M H_2SO_4 devoid of and containing increasing concentrations of compound IV at a scan rate of 50 mV S^{-1}. Similar curves were also obtained for other compounds (I–III).

Inspection of the curves of Fig. 4 reveals that, increasing the concentration of these additives decreases the corrosion current peak (i_p) which suggests the inhibitive effect of these additives.

The inhibition process is assumed to occur via the adsorption of the inhibitor through the lone pair of electrons of the hetero nitrogen atoms and/or the delocalized π-electron of the pyrazole ring [16].

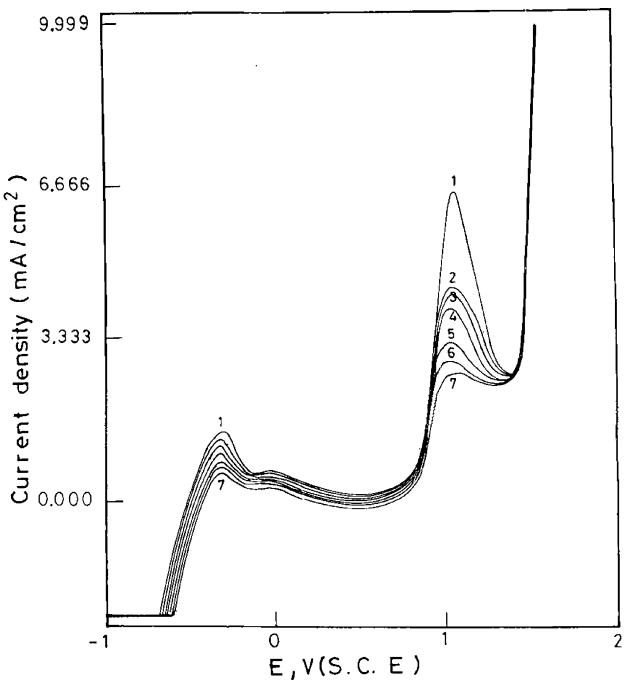

Fig. 4. Potentiodynamic anodic polarization curve of 304 SS in 0.5 M H_2SO_4 containing different concentrations of compound IV at a scan rate of 50 mV s^{-1}: (1) 0.00 M, (2) 1×10^{-5} M, (3) 1×10^{-4} M, (4) 5×10^{-4} M, (5) 1×10^{-3} M, (6) 5×10^{-3} M, (7) 1×10^{-2} M.

Table 4
Effect of inhibitor concentrations on the peak current density (i_p), IE from i_p, anodic charge amount (q_a) and IE from q_a

Inhibitor concentration	i_p (mA cm^{-2})	IE	q_a (mC cm^{-2})	IE
0.5 M H_2SO_4 + compound I				
0.00 M compound I	6.6	–	212.34	–
1×10^{-5} M compound I	4.45	32.57	137.05	35.45
1×10^{-4} M compound I	4.38	33.63	135.38	36.24
5×10^{-4} M compound I	4.18	36.66	126.93	40.22
1×10^{-3} M compound I	3.14	48.48	105.78	50.18
5×10^{-3} M compound I	3.15	52.27	97.18	54.23
1×10^{-2} M compound I	2.48	62.42	73.85	65.22
0.5 M H_2SO_4 + compound II				
1×10^{-5} M compound II	4.38	33.63	136.85	35.55
1×10^{-4} M compound II	4.30	34.84	131.18	38.22
5×10^{-4} M compound II	4.02	39.09	122.83	42.15
1×10^{-3} M compound II	3.30	50.00	99.29	53.24
5×10^{-3} M compound II	2.86	56.66	85.31	59.82
1×10^{-2} M compound II	2.42	63.33	71.72	66.22
0.5 M H_2SO_4 + compound III				
1×10^{-5} M compound III	4.32	34.54	135.64	36.12
1×10^{-4} M compound III	4.20	36.36	130.75	38.42
5×10^{-4} M compound III	3.95	40.15	118.35	44.26
1×10^{-3} M compound III	3.15	52.27	97.20	54.22
5×10^{-3} M compound III	2.52	61.18	77.39	63.55
1×10^{-2} M compound III	2.25	65.90	69.56	67.24
0.5 M H_2SO_4 + compound IV				
1×10^{-5} M compound IV	4.22	36.06	126.93	40.22
1×10^{-4} M compound IV	4.15	37.12	122.83	42.15
5×10^{-4} M compound IV	3.80	42.42	116.02	45.36
1×10^{-3} M compound IV	3.05	53.78	95.17	55.18
5×10^{-3} M compound IV	2.48	62.42	71.72	66.22
1×10^{-2} M compound IV	2.12	67.87	61.85	70.87

The inhibition efficiency (IE) was calculated using the following equation:

$$\mathrm{IE} = 100\left[1 - \frac{i_{p(\mathrm{add})}}{i_{p(\mathrm{free})}}\right] \quad (6)$$

where $i_{p(add)}$ and $i_{p(free)}$ are the peak current densities of peak D in the presence and absence of inhibitors. The values of peak current density and IE are listed in Table 4. From these values, it is clear that: as the concentration of additives increases the value of i_p decreases while the value of IE increases indicating the inhibiting effect of such compounds.

The values of integrated charge amount q_a of the anodic polarization curves was taken also as a measure of IE. The values of q_a are calculated and given in Table 4 and it is clear that, as the added inhibitor concentration increases, the values of q_a decreases. This results indicate the inhibitive effect of these compounds.

The percentage IE of the studied compounds can be calculated from the change of the integrated anodic charge, q_a, in the absence ($q_{a(free)}$) and presence ($q_{a(add)}$) of the inhibitors according to

$$\mathrm{IE} = 100\left(1 - \frac{q_{a(\mathrm{add})}}{q_{a(\mathrm{free})}}\right) \quad (7)$$

The values of IE are given in Table 4. By inspection of the data in Table 4, it is clear that, the efficiency of tested inhibitors from i_p or q_a increases with increasing the inhibitor concentrations. In the presence of one and the same concentration of the added inhibitors, the IE decreases in the following order: compound IV > compound III > compound II > compound I.

3.2. Galvanostatic polarization measurements

Fig. 5 shows the effect of compound IV as an example of addition of 4-substituted pyrazole-5-ones on the anodic and cathodic polarization curves of 304 SS in 0.5 M H_2SO_4 (similar curves were obtained for other compounds). The electrochemical parameters such as corrosion potential ($E_{corr.}$), corrosion current density ($i_{corr.}$) and IE were calculated from the curves of Fig. 5 and given in Table 5. The corrosion current density was determined by the intersection of anodic and cathodic Tafel lines with the steady state (corrosion) potential ($E_{corr.}$).

Table 5
Electrochemical parameters obtained from anodic and cathodic polarization of 304 SS in 0.5 M H_2SO_4 containing different concentrations of inhibitors

Inhibitor concentration	$E_{corr.}$ (mV, SCE)	$i_{corr.}$ (mA cm^{-2})	IE
0.5 M H_2SO_4 + compound I			
0.00 M compound I	−225	5.62	–
1×10^{-5} M compound I	−220	3.72	33.80
1×10^{-4} M compound I	−215	3.68	34.52
5×10^{-4} M compound I	−212	3.60	35.94
1×10^{-3} M compound I	−205	2.94	47.68
5×10^{-3} M compound I	−196	2.62	53.38
1×10^{-2} M compound I	−190	2.12	62.27
0.5 M H_2SO_4 + compound II			
0.00 M compound II	−225	5.62	–
1×10^{-5} M compound II	−220	3.68	34.52
1×10^{-4} M compound II	−217	3.60	35.94
5×10^{-4} M compound II	−210	3.44	38.70
1×10^{-3} M compound II	−204	2.82	49.82
5×10^{-3} M compound II	−192	2.26	59.78
1×10^{-2} M compound II	−188	1.96	65.12
0.5 M H_2SO_4 + compound III			
0.00 M compound III	−225	5.62	–
1×10^{-5} M compound III	−220	3.48	38.07
1×10^{-4} M compound III	−215	3.26	41.99
5×10^{-4} M compound III	−212	3.12	44.48
1×10^{-3} M compound III	−203	2.48	55.87
5×10^{-3} M compound III	−155	1.98	64.76
1×10^{-2} M compound III	−180	1.82	67.61
0.5 M H_2SO_4 + compound IV			
0.00 M compound IV	−225	5.62	–
1×10^{-5} M compound IV	−218	3.56	36.65
1×10^{-4} M compound IV	−210	3.48	38.07
5×10^{-4} M compound IV	−203	3.16	43.77
1×10^{-3} M compound IV	−198	2.54	54.80
5×10^{-3} M compound IV	−190	1.77	68.50
1×10^{-2} M compound IV	−182	1.58	71.88

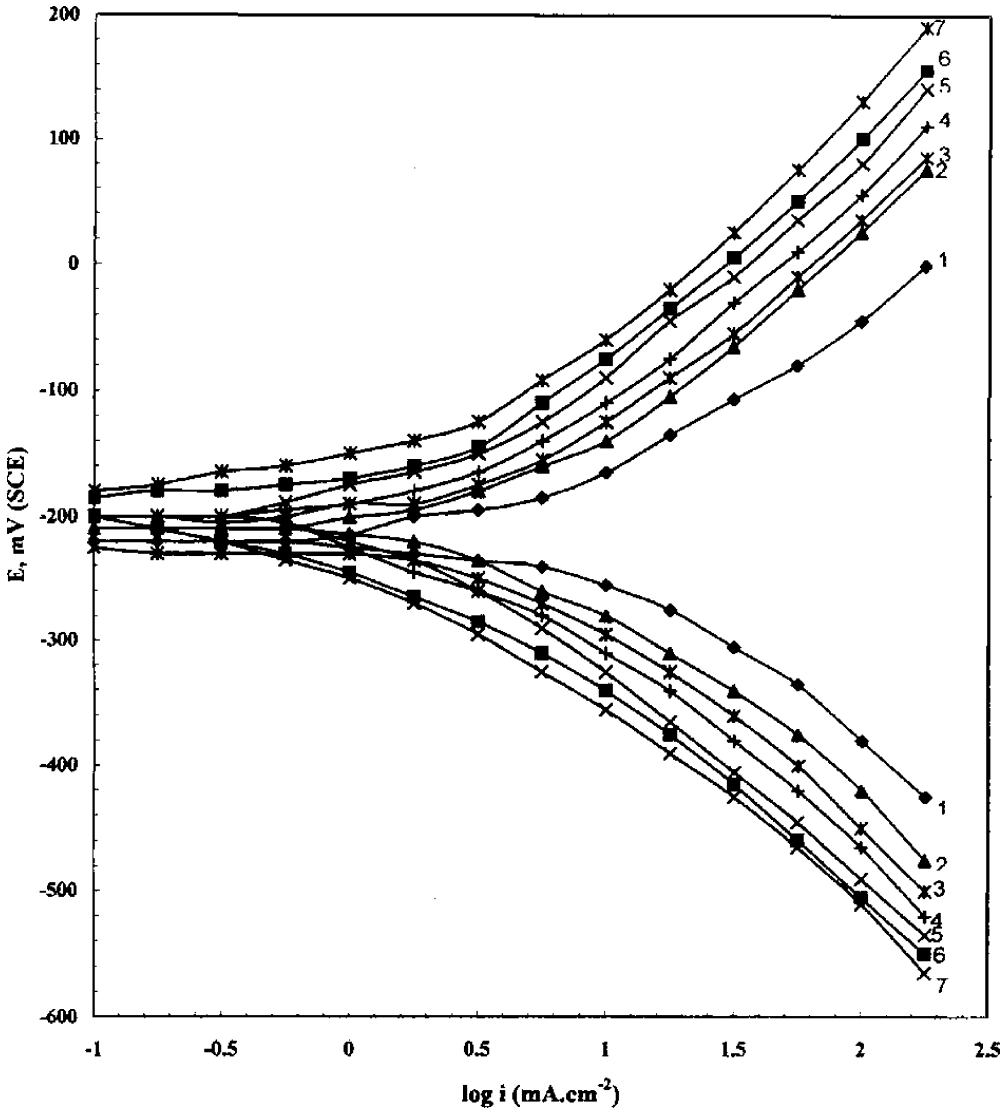

Fig. 5. Anodic and cathodic polarization curves of 304 SS in 0.5 M H_2SO_4 containing different concentrations of compound IV: (1) 0.00 M, (2) 1×10^{-5} M, (3) 1×10^{-4} M, (4) 5×10^{-4} M, (5) 1×10^{-3} M, (6) 5×10^{-3} M, (7) 1×10^{-2} M.

The IE at each concentration was calculated using the equation

$$\mathrm{IE} = \left(1 - \frac{i_{\mathrm{corr.(add)}}}{i_{\mathrm{corr.(free)}}}\right) \times 100 \quad (8)$$

where $i_{\mathrm{corr.(add)}}$ and $i_{\mathrm{corr.(free)}}$ are the corrosion current densities in the presence and absence of inhibitor, respectively.

Inspection of Table 5 reveals that, as the concentration of the additive increases, the corrosion potential is shifted to more positive direction. Moreover, the corrosion current density decreases and the IE increases indicating the inhibitive effect of these compounds. The IE decreases in the following order: compound IV > compound III > compound II > compound I.

The value of IEs which were evaluated for pyrazole-5-one derivatives toward the corrosion of 304 SS in 0.5 M H_2SO_4 using the potentiodynamic anodic polarization curves, amount of anodic charge and galvanostatic polarization show an agreement and conformity of the experimental results. However, there are small difference in the values obtained from the different techniques. This observed discrepancy could be attributed to the differences of the experimental conditions.

3.3. Mechanism of inhibition

4-Substituted pyrazole-5-ones are heterocyclic compounds containing two hetero nitrogen atoms. These atoms act as active adsorption centres at the metal surface. The adsorption bond strength is determined by the electron density of atom acting on the reaction centre and by polarizability of the group [17]. The pyrazole-5-one derivatives used in the present investigation have an electron-donating groups such as $–OCH_3$, $–CH_3CH_2$, CH_3 and electron withdrawing

group such as –Cl. The order of IE of the compounds studied as given by potentiodynamic anodic and galvanostatic polarization techniques, decreases in the following order:

$$–OCH_3 > –CH_3CH_2 > –CH_3 > –Cl$$

The IE among the various additives would originate from the changing nature of substituent in the ring. It is clear from the above sequence that, the compounds containing electron-donating groups are more efficient than that containing electron withdrawing group. The electron-donating group enhances adsorption and subsequent corrosion inhibition a degree dependent on the magnitude of electron charge density on the active centres.

The above order of IE coincides with the electronic factors of these groups as follows. The methoxy group ($–OCH_3$) has a positive mesomeric effect +M and negative inductive effect −I, while the +M is more than −I. So these groups are strong donating groups which increases the localization of the lone pair on nitrogen atoms, i.e. these compounds are easily oxidized and give a polymeric film on the steel electrode as a product of oxidation and consequently the IE increases. In compounds II and III the only factor determine the ease of oxidation is the +I effect which is smaller if compared with the +M effect of compound IV and the order of decreasing inhibition on the steel electrode seems to be logic. On the other hand, compound I (Cl^-) has −I effect and +M effect but the −I > +M. Therefore, electron density on the pyrazole moiety is less than in case of compounds II and III. This leads to a decrease in the IE of these compounds.

4. Conclusion

1. Potentiodynamic anodic polarization curves of 304 SS in 0.5 M H_2SO_4 showed three anodic peaks (A, B and D) and passive region (C) before oxygen evolution.
2. 4-Substituted pyrazole-5-one acts as an inhibitor for corrosion of 304 SS in 0.5 M H_2SO_4.
3. The inhibitive effect of these compounds was attributed to adsorption on the steel surface through the active centre contained in the structure.
4. IE increases with increasing concentrations of the inhibitors as well as its electron donor character of the substituted group.
5. The percentage inhibition efficiencies obtained from both polarization techniques are in good agreement.

References

[1] P.R.P. Rodrinves, I.V. Aoki, A.H.P. DeAndrade, E. De Oliveria, S.M.L. Agostinho, Br. Corros. J. 31 (4) (1996) 305.
[2] A. Kumor, S.P. Borthakur, H.C. Dhawan, Bull. Electrochem. 15 (2) (1999) 63.
[3] X.L. Cheng, H.Y. Ma, S.H. Chen, R. Yn, X. Chen, Z.M. Yao, Corros. Sci. 41 (1999) 321.
[4] R. Agrawal, T.K.G. Namboodhiri, J. Appl. Electrochem. 22 (1992) 383.
[5] M. Abdallah, Corros. Sci. 44 (2002) 717.
[6] F. Bentiss, M. Traisnel, N. Choibi, B. Mernavi, H. Vezin, M. Lagrenee, Corros. Sci. 44 (10) (2002) 2161.
[7] J.G.N. Thomas, Proceedings of the Fifth European Symposium on Corrosion Inhibitors, vol. V, Suppl. No. 8, Ann University, Ferrara, NS Sez., 1980, p. 453.
[8] A.M. Gad Allah, M.M. Hefny, S.A. Salih, M.S. El-Basiouny, Corrosion 45 (7) (1989) 475.
[9] E. Stupnise Ktisac, M. Metikos-Hukovic, D. Lencic, J. Vorkapic-Furac, K. Berkovic, Corrosion 48 (11) (1992) 924.
[10] A.J. Szyproniski, Br. Corros. J. 35 (2) (2000) 155.
[11] A.M. Shams El-Din, S.M. Abd El-Haleem, Werkstoffe Korros. 24 (1973) 389.
[12] N. Ramasnbramanian, N. Preocanin, R.D. Davidson, J. Electrochem. Soc. 132 (4) (1985) 793.
[13] C.R. Clayton, Y.C. Lu, J. Electrochem. Soc. 133 (12) (1986) 2965.
[14] C.J. Chatfield, L.L. Sherier, Corros. Sci. 12 (1972) 563.
[15] W.J. Muller, Trans. Faraday Soc. 27 (1931) 737.
[16] A.G. Gad Allah, M.W. Badawy, H.H. Rehan, M.M. Abou Romia, J. Appl. Electrochem. 19 (1989) 928.
[17] E. Khamis, M. Atea, Corrosion 45 (2) (1994) 106.